Published in final edited form as:
Acta Radiol. 2014 December ; 55(10): 1226–1233. doi:10.1177/0284185113514050.

Rabbit Hepatic Arterial Anatomy Variations: Implications on Experimental Design

Alda L. Tam, M.D.[1], **Marites P. Melancon, Ph.D.**[1], **Joe Ensor, Ph.D.**[2], **Yang Liu, B.S.**[1], **Katherine Dixon, R.T.**[1], **Amanda McWatters, B.S.**[1], and **Sanjay Gupta, M.D.**[1]

[1]Section of Interventional Radiology, Department of Diagnostic Radiology, The University of Texas M.D. Anderson Cancer Center, 1515 Holcombe Blvd., Unit 1471 Houston, Texas 77030; tel: (713) 563-7341; fax: (713) 792-4098

[2]Department of Biostatistics, The University of Texas M.D. Anderson Cancer Center, 1515 Holcombe Blvd., Unit 1411 Houston, Texas 77030; tel: (713) 563-4276; fax: (713) 792-4098

Abstract

Background—The VX2 rabbit model of liver cancer is commonly used to evaluate the efficacy of locoregional anticancer therapy and knowledge of the hepatic arterial anatomy in the rabbit is important for catheter-directed experiments.

Purpose—To describe the normal anatomy and anatomic variations of the celiac axis and hepatic artery in the rabbit.

Material and Methods—Angiograms of 222 rabbits were retrospectively reviewed. The branching pattern of the celiac axis was classified and the diameters of the major branches were measured. Paired t-tests were used to compare the difference between the average sizes of arteries.

Results—Variant celiac axis or hepatic artery anatomy was noted in 25.9% of angiograms, with the gastric branches arising from the proper hepatic artery in 23.3% of cases. The celiac axis could be successfully classified into one of five distinct branching patterns in 193 (86.9%) cases. The mean diameters of the right and left hepatic arteries were 0.67 mm (95% CI [0.64, 0.7]) and 1.25 mm (95% CI [1.19, 1.31]), respectively. The mean diameters of the medial and lateral branches of the left hepatic artery were 0.63 mm (95% CI [0.6, 0.67]) and 0.91 mm (95% CI [0.86, 0.96]), respectively. The right hepatic artery was significantly smaller than the left hepatic artery and the lateral branch of the left hepatic artery (all p-values <0.0001).

Conclusion—Arterial variants in the rabbit are not uncommon. The proper hepatic artery often gives origin to gastric artery branches. To facilitate superselective intra-arterial intervention, the left lateral lobe of the liver should be targeted for tumor implantation because of the significant size difference between the right and left hepatic arteries.

Address reprint requests to: Alda Tam, M.D., Department of Diagnostic Radiology, Unit 1471, The University of Texas M.D. Anderson Cancer Center, PO Box 301402, Houston, Texas 77230-1402. Phone: (713)-563-7920; Fax: (713)-792-4098; alda.tam@mdanderson.org.

The Authors declare that there is no conflict of interest.

Keywords

rabbit; liver angiography; arterial variants; VX2 tumor; liver-directed therapy

Introduction

The VX2 rabbit model of liver cancer is commonly used to evaluate the efficacy of locoregional anticancer therapy (1-5). First described in 1933, VX2 tumor can be induced by the Shope cottontail rabbit papillomavirus and is an anaplastic squamous cell carcinoma (6). Interventional radiologists have found this tumor model to be a useful surrogate in the study of liver directed therapies for hepatocellular carcinoma because VX2 tumor grows rapidly (7), produces lesions large enough to image (1,8) and, like advanced human cancers, is highly glycolytic (9). Furthermore, the hepatic arterial system in the rabbit is similar to that of humans (10) and rabbits are large enough to permit successful intra-arterial catheter manipulations (1,5). However, our knowledge of the rabbit hepatic arterial anatomy has come from a few studies on a limited number of animals (10-12). We present an anatomic classification scheme for the rabbit celiac axis and measurements of the diameters of the major branches based on a review of over 200 angiograms.

Material and Methods

Experimental studies involving rabbits in which angiography was performed from 1994-2013 were reviewed. As this study was a retrospective review of imaging findings, approval from the institution's animal care and use committee was not required. All animals were implanted with VX2 tumor. When the solitary tumor had reached 1 to 2 cm in size, as detected by contrast enhanced computed tomography, angiography was performed as part of the liver directed therapy experiment. All animals with celiac and/or selective hepatic arterial angiograms (n=222) were included in this study. When selective hepatic arterial angiography was performed, the catheter tip was located in the proper hepatic artery. The animal's weight at the time of angiography and the type of catheter used to perform the angiograms were also recorded. All animals were male. An anatomic classification scheme was developed based on the relationship of the origin of the gastroduodenal artery (GDA) from the common hepatic artery (CHA) and the origin of gastric arteries from the proper hepatic artery (PHA). Digital subtraction angiograms were used for evaluation. When the angiograms were on cut films, the films were photographed and digitized for analysis. The diameters of the following arteries were measured: CHA, GDA, proper hepatic artery (PHA), right hepatic artery (RHA), left hepatic artery (LHA), medial branch of the LHA and lateral branch of the LHA. Diameters of the arteries were measured at the following levels: at the level immediately after the origin of the gastric and/or splenic arterial branches but before the origin of the GDA branch for the common hepatic artery, at the level immediately after the origin from the CHA for the GDA, at the level immediately after the origin from the GDA for the PHA, at the level immediately after the origin from the PHA for the RHA, at the level immediately after the origin of the RHA for the LHA, and at the levels immediately after their origins from the LHA for the medial and lateral branches of the LHA. Measurements were obtained using ImageJ, a public domain, Java-based image

processing program developed at the National Institutes of Health (12). To create consistency in the arterial size measurements amongst animals, the size of the catheter used to perform the angiogram was used to set the measurement scale in each animal.

Standard descriptive statistics were used to summarize the frequency of occurrence of the different types of anatomical classifications of the celiac axis. The Pearson's product-moment correlation coefficient and Spearman's rank correlation were calculated for each measured artery to evaluate the bivariate correlation between weight, in kilograms, and artery size, in millimeters. Paired t-tests were used to compare the difference between the average sizes of the right and left hepatic artery and its branches. A p-value of <0.05 was considered statistically significant.

Results

The branching pattern of the celiac axis could be successfully classified into one of five distinct patterns in 193/222 (86.9%) cases. Table 1 summarizes the frequency of occurrence of the different anatomical classifications. The anatomical classification scheme was based on the relationship of the origin of the GDA from the CHA and the origin of gastric arteries from the PHA. Fig. 1 presents a schematic representation of the five distinct patterns. The Type A classification was the most common, occurring in 74.1% of animals. The Type A classification was notable for the GDA arising from the distal portion of the CHA (Fig. 2) and characterized by all gastric branches originating from the CHA. The Type B classifications occurred in 23.3% of animals and were associated with the origin of the GDA arising from the proximal portion of the CHA. In Type B1, the CHA segment could be effectively separated from the origin of the GDA (Fig. 3a). In Type B2, the CHA could not be separated from the origin of the GDA or the origin of the splenic artery, and represents, in essence, a trifurcation of the celiac axis (Fig. 3b). In both Type B1 and B2 classifications, gastric arterial branches could be found to originate from the PHA distal to the origin of the GDA. In Type C, the hepatic artery originated from the superior mesenteric artery and the GDA originated from the celiac axis (Fig. 4). In Type D, the GDA arose off a gastric arterial branch and not the CHA (Fig. 5). Types C and D were seen in less than 3% of animals.

The average weight of the rabbits was 3.67 kg (95% CI [3.60, 3.75], range 2.7 kg to 4.69 kg). There was no correlation between weight and size of the CHA ($p=0.73$), GDA ($p=0.92$), PHA ($p=0.98$), RHA ($p=0.60$), LHA ($p=0.11$), medial branch of the LHA ($p=0.13$), or lateral branch of the LHA ($p=0.19$). Table 2 summarizes the size of the major arterial branches of the celiac axis in millimeters. As the ability to subselectively catheterize the arteries feeding the tumor is important, the size of the RHA was compared with the size of the LHA and its branches. The mean diameter of the RHA was 0.67 mm (95% CI [0.64, 0.7]). The mean diameter of the LHA was 1.25 mm (95% CI [1.19, 1.31]). The mean diameters of the medial and lateral branches of the LHA were 0.63 mm (95% CI [0.6, 0.67]) and 0.91 mm (95% CI [0.86, 0.96]), respectively. The RHA was significantly smaller than the LHA and the lateral branch of the LHA (all p-values <0.0001).

Discussion

The hepatic VX2 tumor model in the rabbit is important for imaging and translational interventional oncology research. However, angiography, particularly superselective catheterization, in the rabbit can be challenging because the rabbit vessels are small and tortuous (12,14) and prone to long-lasting, drug-resistant spasm (14,15). Knowledge about the rabbit celiac axis and hepatic arterial anatomy can help to improve the reliability of the tumor model and ensure the success of experimental studies. Therefore, we report our findings on the branching patterns of the celiac axis and the diameter measurements of its major hepatic branches.

While we found the most common branching pattern of the celiac axis (Type A) to be the same as the one described by Seo et al.(11), we discovered three additional branching patterns (Type B1, Type B2 and Type D) that have not been previously described. The detection of additional celiac axis anatomy variants was expected as our study involved the review of over 200 rabbit angiograms as compared to the Seo et al. (11) study which was completed on 24 rabbits. The Type B classifications, which occurred in 23% of the rabbits and are characterized by a short segment CHA or a trifurcation of the celiac axis, are important because gastric branches may originate from the PHA distal to the origin of the GDA. The ability to recognize arterial branches supplying the gastrointestinal tract is central to preventing non-target embolization as this is not well tolerated in the rabbit. Burgener and Göthlin noted that the improper placement of the catheter into the PHA resulting in reflux of even small amounts of embolic material into the GDA or gastric branches would results in stomach perforation and death within 2-4 days (10).

In their 2009 paper, Lee et al. (12) noted that the implantation of VX2 tumor into the left lateral lobe of the liver facilitated successful superselective hepatic arterial catheterization and chemoembolization. They attributed this to a more favorable angle of origin and a longer length of the lateral branch of the LHA compared to the medial branch of the LHA (12). The findings in our study lend support to their conclusions by demonstrating significant size differences between the RHA, medial branch of the LHA and lateral branch of the LHA. We found the mean diameters of the LHA and the lateral branch of the LHA, which were 1.25 mm and 0.91 mm, respectively, to be of a size that would easily accommodate microcatheters up to 2.4 French (0.8 mm outer diameter) in size. In contrast, the mean diameters of the RHA and the medial branch of the LHA, which were 0.67 mm and 0.63 mm, respectively, make it likely that even a 2 French (0.67 mm outer diameter) microcatheter would be occlusive. Furthermore, the acute angles of origin and the small size of the RHA and medial branch of the LHA preclude consistent, successful selective catheterization for liver directed therapy thereby constraining the use of the right lobe and left medial lobe of the liver as tumor implantation sites. Therefore, we concur with Lee et al. (12) that the left lateral lobe of the liver should be used as a site for tumor implantation to facilitate superselective intra-arterial intervention.

This study is limited by its retrospective nature and the inability to correlate the angiographic findings with pathologic specimens. In addition, all the rabbits were male, raising the possibility that we failed to detect a difference in hepatic arterial size based on

the sex of the animal. While there was no difference in the diameter of the celiac axis, a recent study did describe a significant difference in the arterial diameters of the left cranial abdominal artery and the caudal mesenteric artery of male versus female New Zealand white rabbits (16). This study also does not include an experimental component to evaluate whether subselective catheterization of the RHA would be as difficult as we surmise. While it would be ideal to a comparison of the rates of successful subselective catheterization and tumor embolization from the right versus left hepatic arteries, this would not be a practical experiment. Most investigators use an open surgical technique, where a subxyphoid laparotomy is performed and the left lobe of the liver is extirpated, for tumor implantation as it is easier to access the left lobe rather than the right lobe of the liver (17-19). Lastly, it is possible that implantation of the VX2 tumor in to the left lateral lobe of the liver contributed to hypertrophy of the LHA and its branches; however, given that the tumors were only 1 to 2 cm in size at the time of angiography, we suspect the degree of hypertrophy to be minimal.

VX2 in the rabbit liver is a useful tumor model for evaluating liver directed therapies and while there have been studies that have looked at optimizing implantation techniques (17-19), there is little in the modern literature (11,12) that looks at improving the model from an anatomical perspective. This study provides a detailed classification of the branching pattern of the celiac axis in the rabbit, including three variations that have not been previously described; a quantitative evaluation of the size of major hepatic arterial branches; and, practical points for investigators to help with the design and execution of trans-arterial liver directed therapies.

In conclusion, variations in the celiac artery branching patterns and hepatic artery anatomy in rabbits are not uncommon, with the proper hepatic artery giving origin to gastric artery branches in many cases. It is important to know and recognize these variations in hepatic artery embolization or chemoembolization experiments; in these situations, the catheter needs to be positioned beyond the origin of the gastric branches to minimize the risk of non-target embolization to the gastrointestinal tract. In addition, the LHA and lateral branch of the LHA are generally of a size that will permit the use of microcatheters up to 2.4 French in size for selective catheterization; hence, if the experiment requires superselective catheterization, the optimal site for tumor implantation is the left lateral lobe of the rabbit liver.

Acknowledgments

This research received no specific grant from any funding agency in the public, commercial, or not-for-profit sectors.

References

1. Geschwind JF, Artemov D, Abraham S, et al. Chemoembolization of liver tumor in a rabbit model: assessment of tumor cell death with diffusion-weighted MR imaging and histologic analysis. J Vasc Interv Radiol. 2000; 11:1245–1255. [PubMed: 11099235]
2. Hong K, Kobeiter H, Georgiades CS, et al. Effects of the type of embolization particles on carboplatin concentration in liver tumors after transcatheter arterial chemoembolization in a rabbit model of liver cancer. J Vasc Interv Radiol. 2005; 16:1711–1717. [PubMed: 16371540]

3. Izumi B, Tashiro S, Miyauchi Y. Anti-cancer effects of local administration of mitomycin C via the hepatic artery or portal vein on implantation and growth of VX2 cancer injected into rabbit liver. Cancer Res. 1986; 46:4167–4170. [PubMed: 3089588]
4. Virmani S, Wang D, Harris KR, et al. Comparison of transcatheter intra-arterial perfusion MR imaging and fluorescent microsphere perfusion measurements during transcatheter arterial embolization of rabbit liver tumors. J Vasc Interv Radiol. 2007; 18:1280–1286. [PubMed: 17911519]
5. Geschwind JF, Ko YH, Torbenson MS, et al. Novel therapy for liver cancer: direct intraarterial injection of a potent inhibitor of ATP production. Cancer Res. 2002; 62:3909–3913. [PubMed: 12124317]
6. Shope RE, Hurst EW. Infectious papillomatosis of rabbits. J Exp Med. 1933; 58:607–624. [PubMed: 19870219]
7. Kuszyk BS, Boitnott JK, Choti MA, et al. Local tumor recurrence following hepatic cryoablation: radiologic-histolopathologic correlation in a rabbit model. Radiology. 2000; 217:477–486. [PubMed: 11058649]
8. Wang D, Bangash AK, Rhee TK, et al. Monitoring embolization in rabbits with VX2 tumors-transcatheter intraarterial first-pass perfusion MR imaging. Radiology. 2007; 245:130–139. [PubMed: 17885186]
9. Arora KK, Pedersen PL. Functional significance of mitochondrial bound hexokinase in tumor cell metabolism: evidence for preferential phosphorylation of glucose by intramitochondrially generated ATP. J Biol Chem. 1988; 263:17422–17428. [PubMed: 3182854]
10. Burgener FA, Gothlin JH. Angiographic, microangiographic and hemodynamic evaluation of hepatic artery embolization in the rabbit. Invest Radiol. 1978; 13:306–312. [PubMed: 689823]
11. Seo TS, Oh JH, Lee DH, et al. Radiologic anatomy of the rabbit liver on hepatic venography, arteriography, portography, and cholangiography. Invest Radiol. 2001; 36:186–192. [PubMed: 11228583]
12. Lee KH, Liapi E, Buijs M, et al. Considerations for implantation site of VX2 carcinoma into rabbit liver. J Vasc Interv Radiol. 2009; 20:113–117. [PubMed: 19028118]
13. Image J (rsb.info.nih.og/ij/; 1.47i downloaded 1/25/2013)
14. Kónya A, Wright KC, Szwarc IA, et al. Technical aspects of catheter-related interventions in the liver of the rabbit. Acta Radiol. 1997; 38:332–334. [PubMed: 9093176]
15. Jensen R, Olin T. Balloon catheters in angiography: an experimental investigation in rabbits. Acta Radiol Diagn (Stockh). 1972; 12:721–736. [PubMed: 4651748]
16. Ahasan ASML, Islam MS, Kabria ASMG, et al. Major variation in branches of the abdominal aorta in New Zealand white rabbit (*Orycotolagus Cuniculus*). International Journal of Natural Sciences. 2012; 2:91–98.
17. Chen JH, Lin YC, Huang YS, et al. Induction of VX2 carcinoma in rabbit liver: comparison of two inoculation methods. Lab Anim. 2004; 38:79–84. [PubMed: 14979992]
18. Lee KH, Liapi E, Buijs M, et al. Percutaneous US-guided implantation of Vx-2 carcinoma into rabbit liver: a comparison with open surgical method. J Surg Res. 2009; 155:94–9. [PubMed: 19181344]
19. Virmani S, Harris KR, Szolc-Kowalska B, et al. Comparison of two different methods for inoculating VX2 tumors in rabbit livers and hind limbs. J Vasc Interv Radiol. 2008; 19:931–936. [PubMed: 18503910]

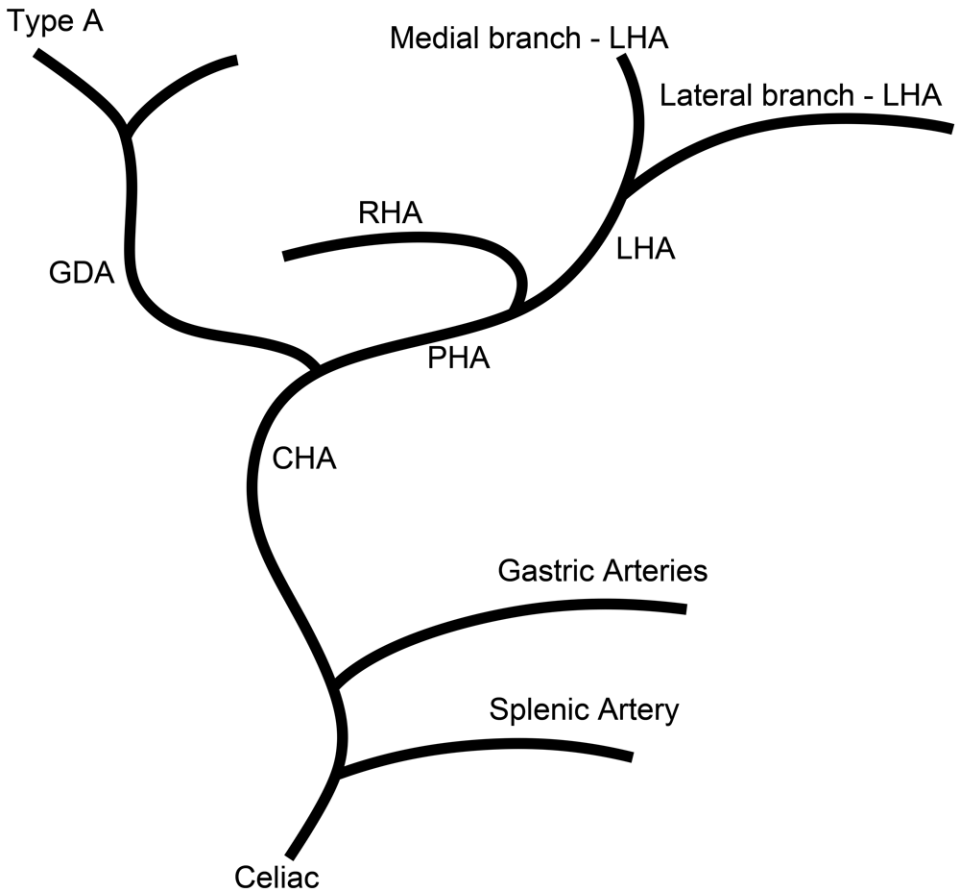

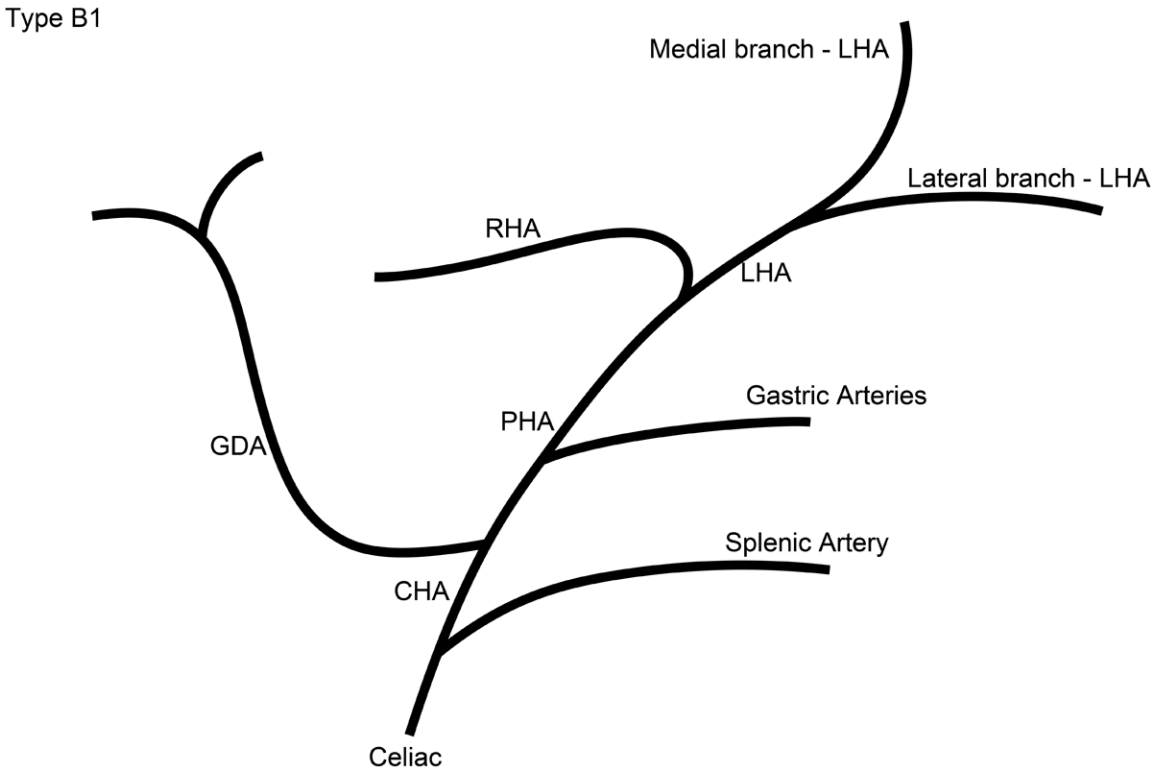

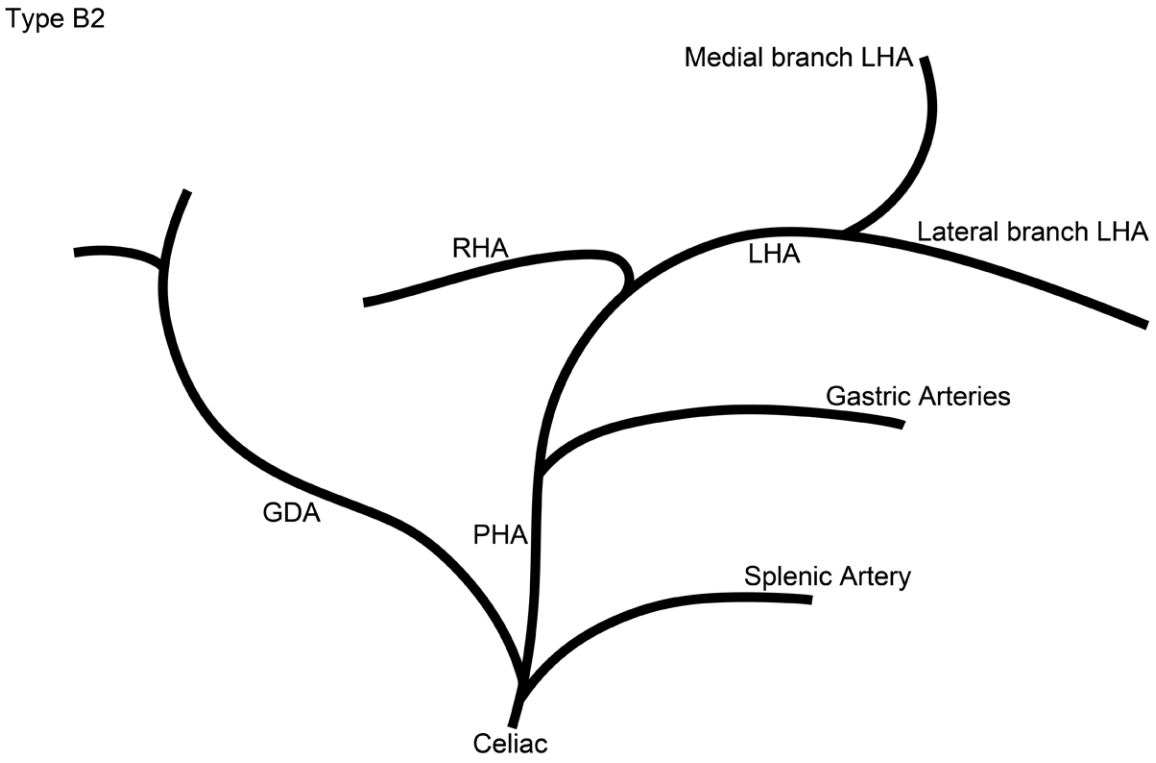

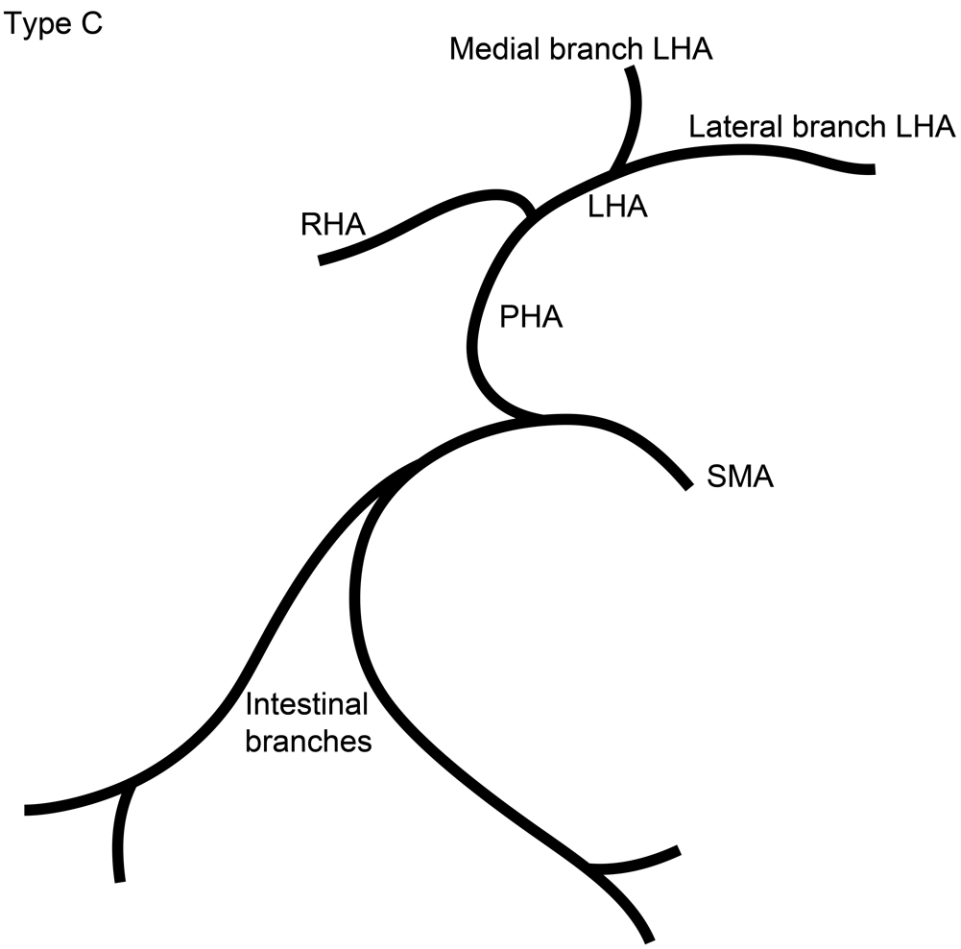

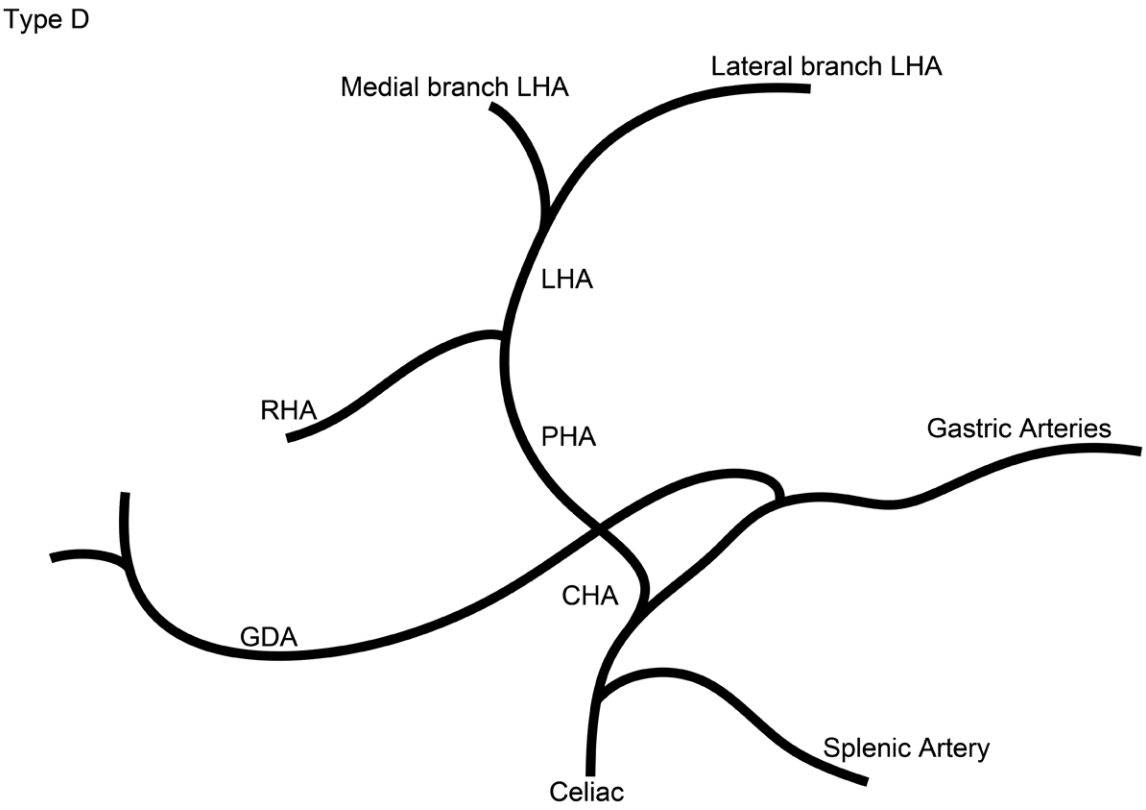

Fig. 1.

Schematic representation of the five different branching patterns of the rabbit celiac axis. (A) Type A is the most common branching pattern and characterized by the gastroduodenal artery (GDA) arising off the distal portion of the common hepatic artery (CHA) and all gastric arterial branches arising off of the CHA. (B) Type B1 is characterized by the GDA arising off the proximal portion of the CHA and gastric arterial branches arising from both the CHA and the proper hepatic artery (PHA). (C) In Type B2, the CHA cannot be clearly identified as a distinct segment and represents a trifurcation of the celiac axis into the splenic/gastric arteries, the CHA and the GDA. Gastric arterial branches may also arise from the PHA. (D) Type C represents the variation where the PHA arises from the superior mesenteric artery (SMA) and not the celiac axis. (E) Type D represents the variation where the GDA does not arise from the CHA, instead coming off of a gastric arterial branch.

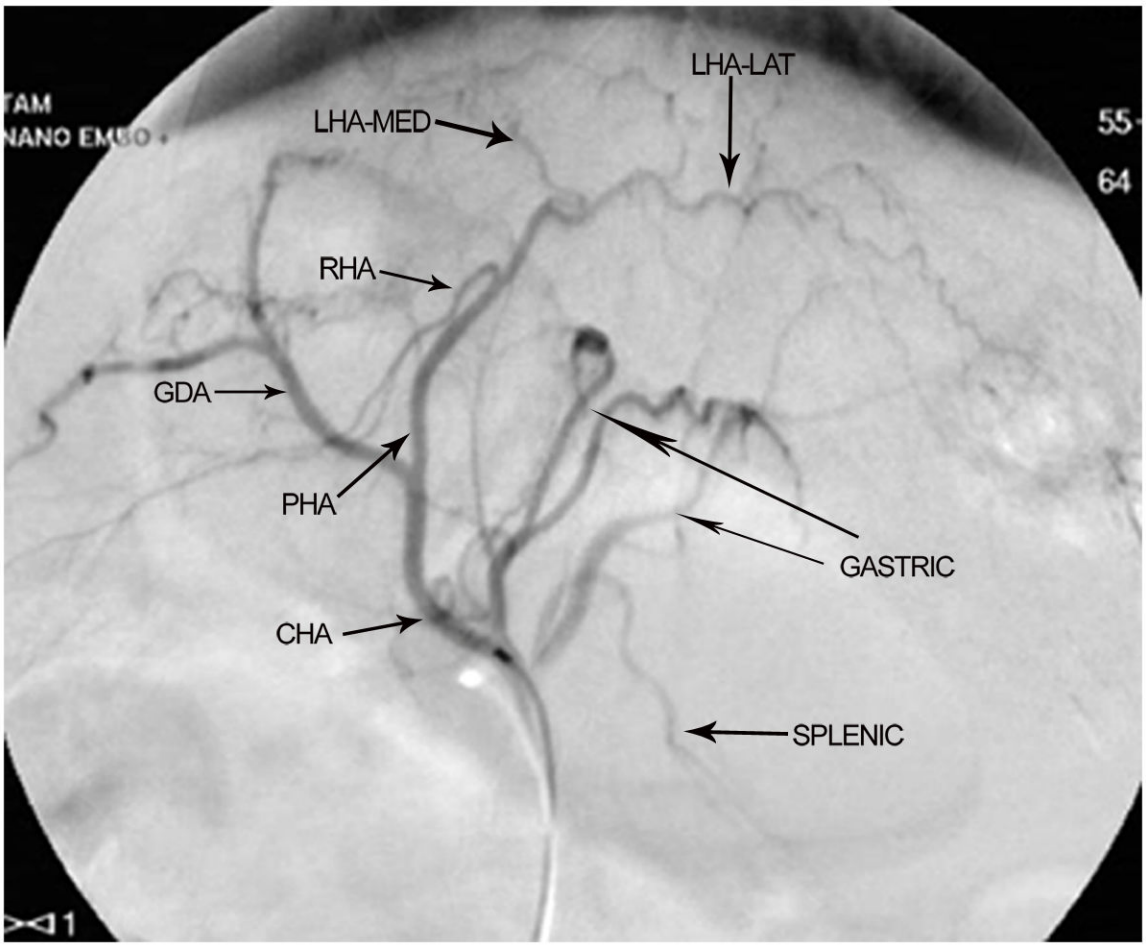

Fig. 2.

Digital subtraction angiography demonstrating anatomical classification Type A. After the origins of the gastric and splenic arterial branches, the gastroduodenal artery (GDA) arises off the distal segment of the common hepatic artery (CHA). The right hepatic artery (RHA) and the medial branch of the left hepatic artery (LHA-med) originate at acute angles when compared with the lateral branch of the left hepatic artery (LHA-lat). Proper hepatic artery (PHA).

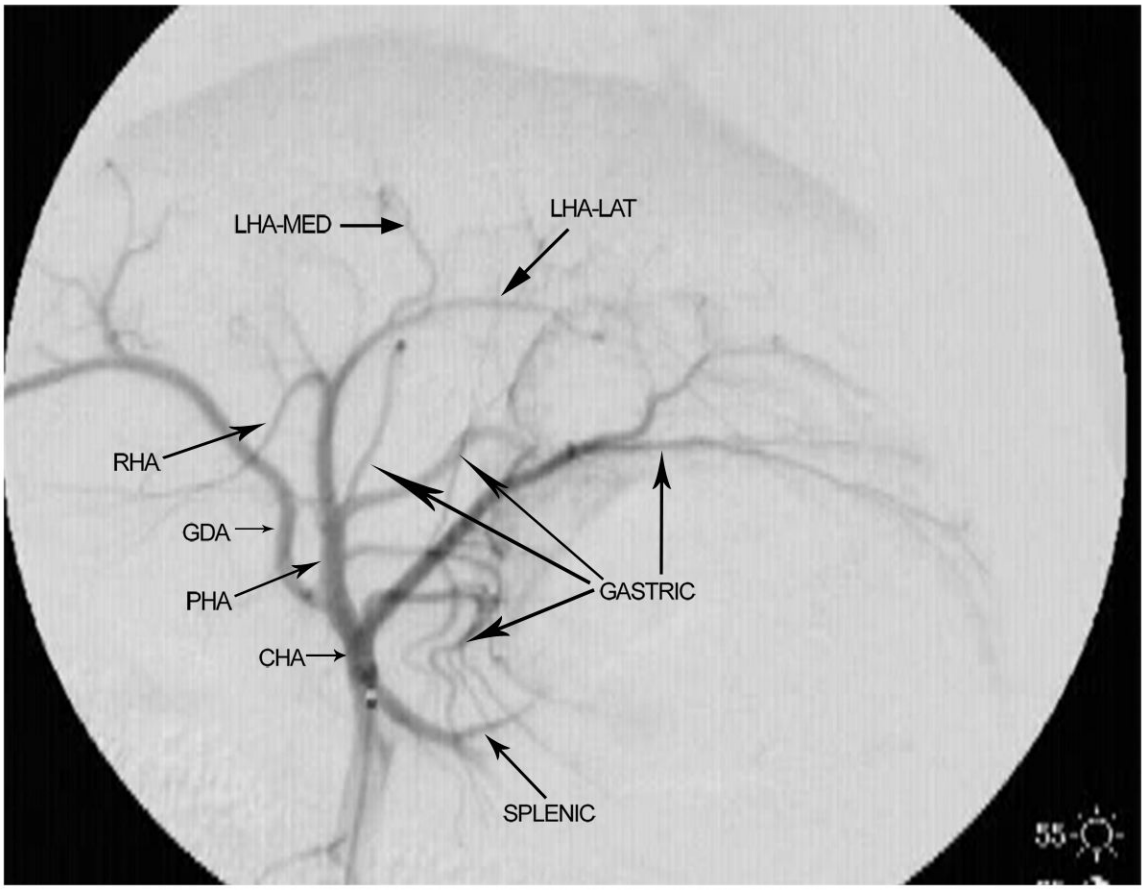

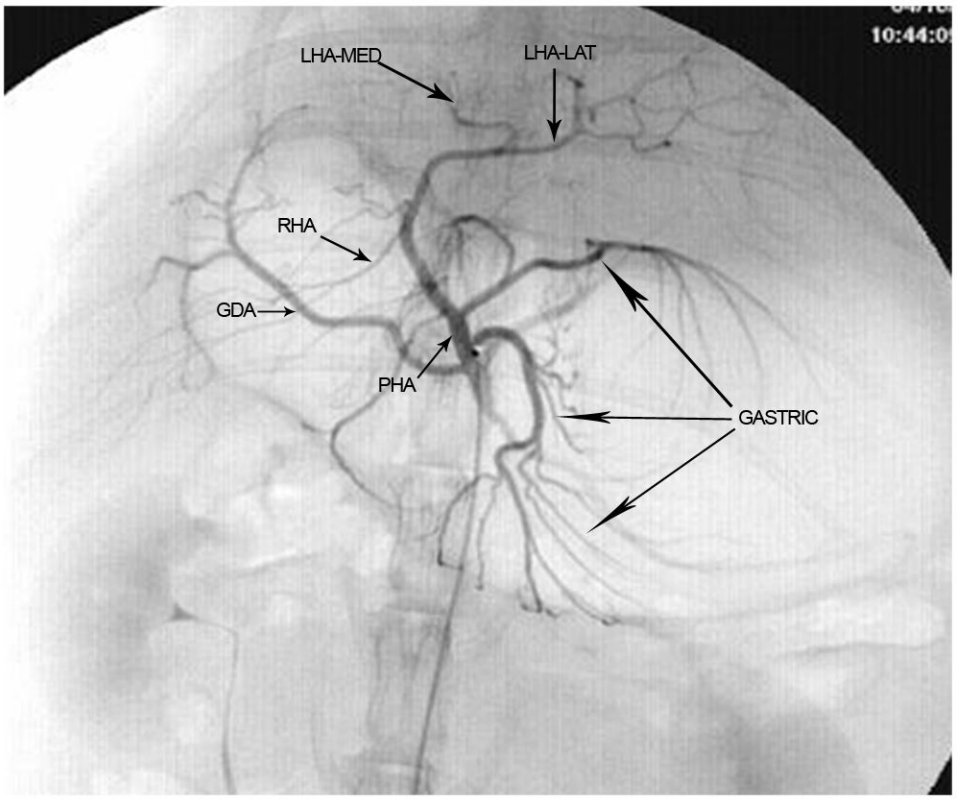

Fig. 3.

a) Digital subtraction angiography demonstrating anatomical classification Type B1. The gastroduodenal artery (GDA) arises off the proximal portion of the common hepatic artery (CHA). Gastric arterial branches originate from the proper hepatic arterial (PHA) segment distal to the origin of the GDA. The right hepatic artery (RHA) and the medial branch of the left hepatic artery (LHA-med) originate at acute angles when compared with the lateral branch of the left hepatic artery (LHA-lat). b) Digital subtraction angiography demonstrating anatomical classification Type B2. The common hepatic artery (CHA) cannot be clearly delineated as a separate segment. The celiac axis trifurcates into the splenic/gastric arterial branches, the CHA and the gastroduodenal artery (GDA). Gastric arterial branches may originate from the proper hepatic arterial (PHA) segment distal to the origin of the GDA. The right hepatic artery (RHA) and the medial branch of the left hepatic artery (LHA-med) originate at acute angles when compared with the lateral branch of the left hepatic artery (LHA-lat).

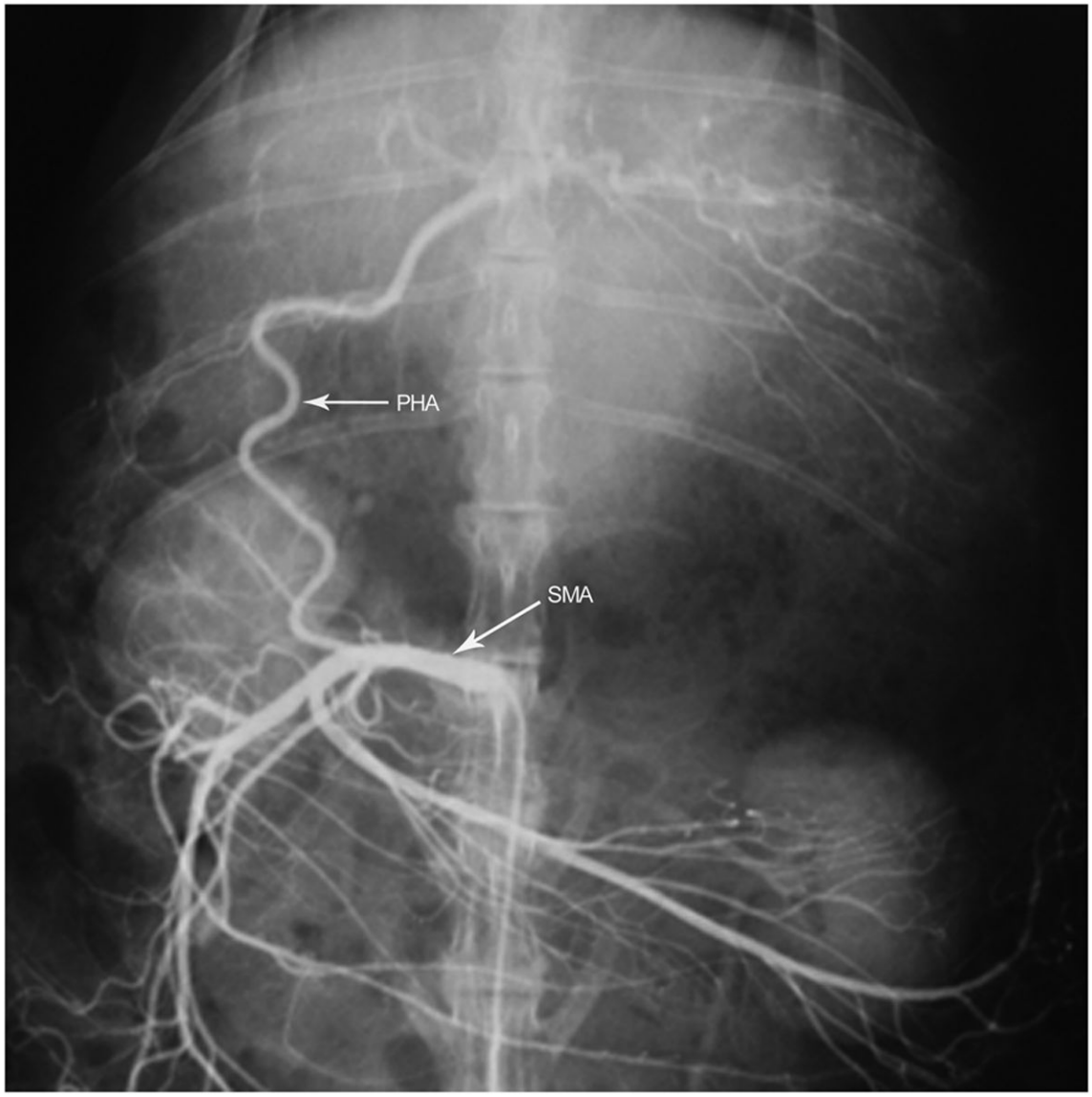

Fig. 4.

Angiogram of the superior mesenteric artery demonstrating anatomical classification Type C where the proper hepatic artery (PHA) arises as a branch off the superior mesenteric artery (SMA). The gastroduodenal artery, gastric arterial branches and splenic artery are branches of the celiac axis (celiac angiogram not shown).

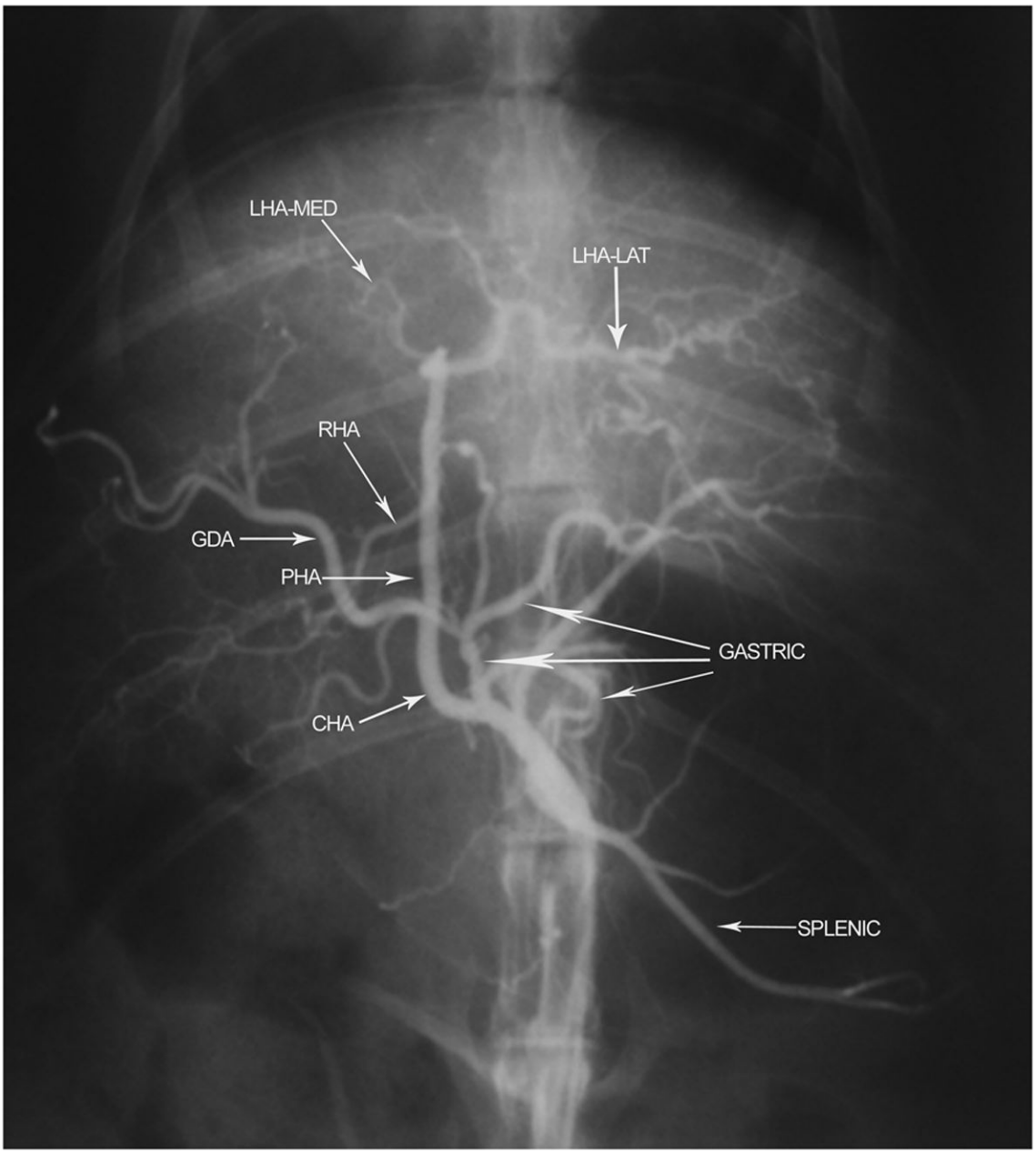

Fig. 5.

Angiogram of the celiac axis demonstrating anatomical classification Type D. The common hepatic artery (CHA) gives rise to the gastric and splenic arterial branches before continuing as the proper hepatic artery (PHA). The gastroduodenal artery (GDA) does not arise from the CHA but instead originates from a gastric arterial branch. Right hepatic artery (RHA); medial branch of left hepatic artery (LHA-med); lateral branch of left hepatic artery (LHA-lat).

Table 1
Frequency of Occurrence of Different Anatomical Classifications

Anatomical Classification	Frequency (%)
Type A	143 (74.1)
Type B1	17 (8.8)
Type B2	28 (14.5)
Type C	3 (1.6)
Type D	2 (1.0)
Total	**193 (100)**

Table 2

Size of Major Arterial Branches of the Celiac Axis in Millimeters (mm)

Artery							95% CI for Mean	
	N	Mean	Median	Std Dev	Minimum	Maximum	Lower	Upper
Common Hepatic	166	2.19	2.17	0.69	0.65	4.11	2.09	2.30
Gastroduodenal	197	1.76	1.61	0.66	0.52	3.79	1.66	1.85
Proper Hepatic	218	1.68	1.62	0.55	0.51	3.56	1.60	1.75
Right Hepatic	206	0.67	0.62	0.22	0.25	1.56	0.63	0.69
Left Hepatic	220	1.25	1.21	0.46	0.49	2.65	1.19	1.32
Left Medial Branch	192	0.63	0.59	0.24	0.26	1.37	0.60	0.67
Left Lateral Branch	205	0.91	0.84	0.34	0.37	1.95	0.87	0.96